JCTC Journal of Chemical Theory and Computation

Article

pubs.acs.org/JCTC

Can the Closed-Shell DFT Methods Describe the Thermolysis of 1,2-Dioxetanone?

Ling Yue,[†] Daniel Roca-Sanjuán,[‡] Roland Lindh,[‡] Nicolas Ferré,[§] and Ya-Jun Liu*[,†]

[†]Key Laboratory of Theoretical and Computational Photochemistry, Ministry of Education, College of Chemistry, Beijing Normal University, Beijing 100875, China

[‡]Department of Chemistry—Ångström, The Theoretical Chemistry Programme, Uppsala University, P.O. Box 518, S-75120 Uppsala, Sweden

[§]Université d'Aix-Marseille, Institut de Chimie Radicalaire, 13397 Marseille Cedex 20, France

Supporting Information

ABSTRACT: The chemiluminescent decomposition of 1,2-dioxetanone has in the past been studied by state-of-the-art multireference quantum chemical calculations, and a stepwise biradical mechanism was established. Recently, this decomposition has been reinvestigated, and a concerted mechanism has been proposed based on calculations performed at the closed-shell density functional theory (DFT) level of theory. In order to solve this apparent mechanistic contradiction, the present paper presents restricted and unrestricted DFT results obtained using functionals including different amounts of Hartree−Fock (HF) exchange, repeating and complementing the above-mentioned DFT calculations. The calculated results clearly indicate that the closed-shell DFT methods cannot correctly describe the thermolysis of 1,2-dioxetanone. It is found that unrestricted Kohn−Sham reaction energies and barriers are always lower than the ones obtained using a restricted formalism. Hence, from energy principles, the biradical mechanism is found to be prevailing in the understanding of the 1,2-dioxetanone thermolysis.

INTRODUCTION

The thermolysis of peroxide is the key step for nearly all of the organic chemiluminescence processes.[1] The decomposition of 1,2-dioxetanone (see Chart 1), a small analogue of firefly dioxetanone, has been studied using state-of-the-art quantum chemical calculations (note that the size of the active space was verified to be sufficient[2]), and it was concluded that a stepwise biradical mechanism is the most probable reaction path.[3] Our recent study, combining second-order multiconfigurational perturbation (CASPT2) and coulomb attenuated hybrid exchange-correlation functional (CAM-B3LYP) methods to investigate the decomposition of firefly dioxetanone also indicated the same stepwise biradical mechanism.[4] However, da Silva and da Silva revisited the decomposition of 1,2-dioxetanone using restricted Kohn−Sham density functional theory (DFT) calculations and suggested a concerted mechanism in association with a MPWB1K functional (contains 44% exact HF exchange).[5] The concerted[5] and stepwise biradical[3,4] mechanism were depicted in Scheme 1. Accordingly, visual inspection (not based on calculation) of the potential energy curve (PEC) of the closed-shell ground state (S_0) shows crossings with the PECs of the first (T_0) and second (T_1) triplet states twice (for convenient comparison, we use the notations in ref 5), but not with the PEC of the first singlet excited state (S_1). Moreover, there is an intersystem crossing (ISC) between the S_1 and T_1 PECs, which can be the reason for the formation of products in the S_1 PEC as da Silva and da Silva stated.[5] On the basis of the above findings, they rationalized the experimental result that the yield of the fluorescence is much lower than the phosphorescence. Their results and conclusion have been questioned by Roca-Sanjuán et al.[6] da Silva and da Silva responded to these comments immediately[7] mainly by saying that "the suggested reaction mechanism was in line with experimental findings". In this paper, we will not try to explain the experimental findings, the predominance of the triplet-state products, and the inefficiency of the chemiexcitation mechanism. From the viewpoint of the employed methodology, we would like to tell the fact that the results presented in ref 5 do not directly provide evidence in favor or disfavor of the concerted or stepwise biradical mechanism. We only want to answer one question: whether the closed-shell DFT methods, in association with functionals with a large quantity of exact HF exchange, can correctly describe the thermal decomposition of 1,2-dioxetanone. If so, the discussion of da Silva et al. is based on reasonable calculated results. If not, the proposed concerted mechanism is not supported by theoretical results. In this contribution, we will sort this out in some detail.

Chart 1. 1,2-Dioxetanone and Firefly Dioxetanone

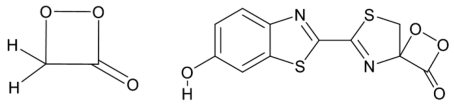

1,2-dioxetanone Firefly dioxetanone

Received: July 26, 2012
Published: September 12, 2012

   dx.doi.org/10.1021/ct3006562 | J. Chem. Theory Comput. 2012, 8, 4359−4363

Scheme 1. The Concerted and Step-Wise Biradical Decomposition of 1,2-Dioxetanone

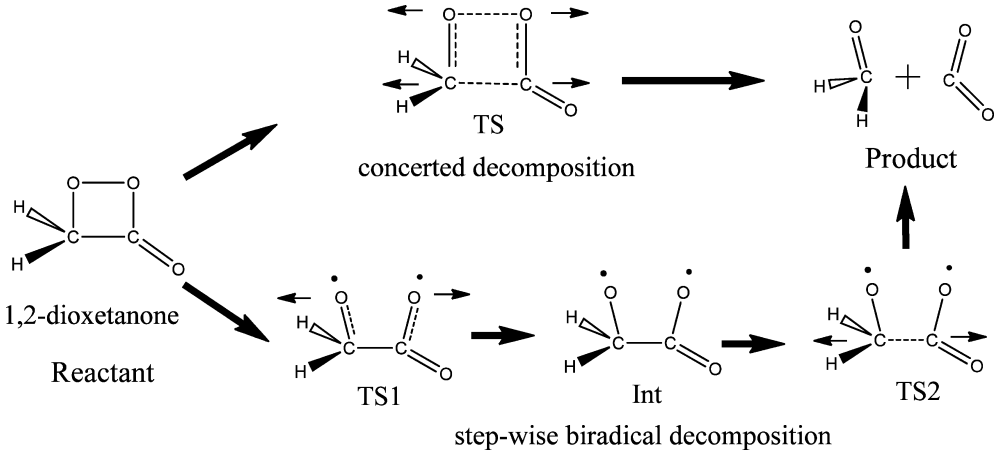

COMPUTATIONAL DETAILS

According to the hybrid generalized gradient approximation, for instance Becke's three parameter hybrid functional,[8] the DFT exchange-correlation energy can be expressed as

$$E_{XC} = p_2 E_X^{HF} + p_1(p_4 E_X^{local} + p_3 \Delta E_X^{nonlocal}) + p_6 E_C^{local} + p_5 \Delta E_C^{nonlocal}$$

where E_X^{HF} is the Hartree−Fock (HF) exchange energy, E_X^{local} and $E_X^{nonlocal}$ are the local and nonlocal exchange energies, respectively, and E_C^{local} and $\Delta E_C^{nonlocal}$ are the local and nonlocal correlation energies, respectively. In the B3LYP functional,[8,9] the Slater local and Becke nonlocal exchange functionals are used. In addition, Vosko, Wilk, and Nusair local correlation (VWN) and Lee, Yang, and Parr (LYP) nonlocal correlation are used as the local and nonlocal correlation functionals, respectively. That is, the standard B3LYP functional is expressed as

$$E_{XC} = 0.20E_X^{HF} + 1.00(0.80E_X^{Slater} + 0.72\Delta E_X^{Becke}) + E_C^{VWN} + 0.81\Delta E_C^{LYP}$$

In the above equation, the parameter p_2 denotes the amount of HF exchange contained in the exchange correlation energy. In this study, we use five functionals with different percentages of HF exchange by modifying p_1 and p_2 parameters (see Table 1) to study the effect of the inclusion of large quantities of exact exchange. All the ground-state geometry optimizations, frequency analyses, and calculations of intrinsic reaction coordinate (IRC) were performed using the density functionals in Table 1 and the best five functionals stated in ref 5. The restricted closed-shell DFT methods in Table 1 were used to locate the TS of the decomposition of 1,2-dioxetanone and calculate the corresponding IRC paths. The T_0 energy was calculated using ground state IRC structures at the same level of theory. We tested the stability of the wave function along all the S_0 and T_0 PECs. The instability of the wave function can be due to (1) restricted to unrestricted spin instabilities, (2) symmetric to unsymmetric solutions of the wave function, and (3) the solution of the optimization of the wave function corresponding to a transition state in the space of the wave function parameters.[10] The molecular systems studied here have no symmetry elements, hence instabilities of type 2 do not exist. In the case of instabilities of type 1, the wave function should be reoptimized with an unrestricted spin constraint. Instabilities of type 3 indicate that the computed wave function does not correspond to a local minimum and is not computed in the spirit of the variational principle. These results should be discarded. The reaction barrier was calculated as the variation of the Gibbs free energy (ΔG) between the transition state and the reactant. To consider the influence of the solvent, the polarizable continuum model (PCM)[11] for the nonpolar solvent, benzene, and the conductor-like polarized continuum model (C-PCM)[12] for the polar solvent, dichloromethane and dimethyl sulfoxide (DMSO) were employed. The same solvents were considered in ref 5. The aug-cc-pVDZ basis set[13] was used for all calculations, which is also the largest basis set employed in the previous calculations. All the present calculations were performed with the Gaussian 09 program suite.[14]

Table 1. The DFT Calculated Reaction Barrier ΔG (kcal/mol) of the Concerted (Using Closed-Shell Approach) and Step-Wise Biradical Decomposition (Using Open-Shell Approach) of the Decomposition of 1,2-Dioxetanone[a]

functional-HF amount (in %)	p_1	p_2	concerted	biradical
BLYP-20 (B3LYP)	1.00	0.20	26.0	17.5
BLYP-40	0.80	0.40	37.6	15.8
BLYP-60	0.60	0.60	48.8	13.3
BLYP-80	0.40	0.80	59.6	11.4
BLYP-100	0.20	1.00	69.6	10.1

[a]The p_1 and p_2 parameters are defined in the Computational Details section.

RESULTS AND DISCUSSION

The S_0 energetics along the reaction path are shown in Figure 1. We observe that the reaction barrier increases with increasing percentage of HF exchange in the functional. The ΔG difference between BLYP-20 and BLYP-100 is as large as 43.6 kcal/mol, as indicated in Table 1. Actually, stability calculations demonstrate that these large ΔG values mainly originate from a restricted → unrestricted instability of the Kohn−Sham Slater determinant. The larger the amount of HF exchange in the functional, the more instable the wave function, as is clearly shown in Figure 2. While the profiles obtained with BLYP with 20% HF exchange, i.e., B3LYP, are not significantly different, the others featuring a larger amount of HF exchange are different, demonstrating an instability of the closed shell

dx.doi.org/10.1021/ct3006562 | J. Chem. Theory Comput. 2012, 8, 4359−4363

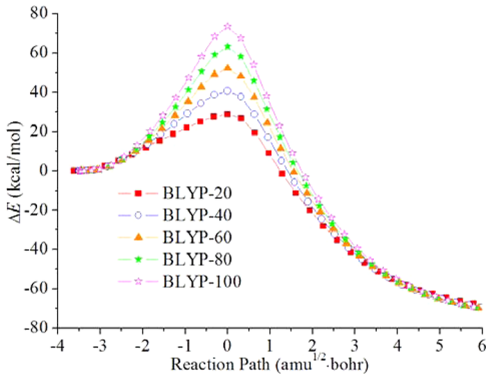

Figure 1. The energy profiles of the S_0 state calculated by the closed-shell DFT methods with different percentages of HF exchange.

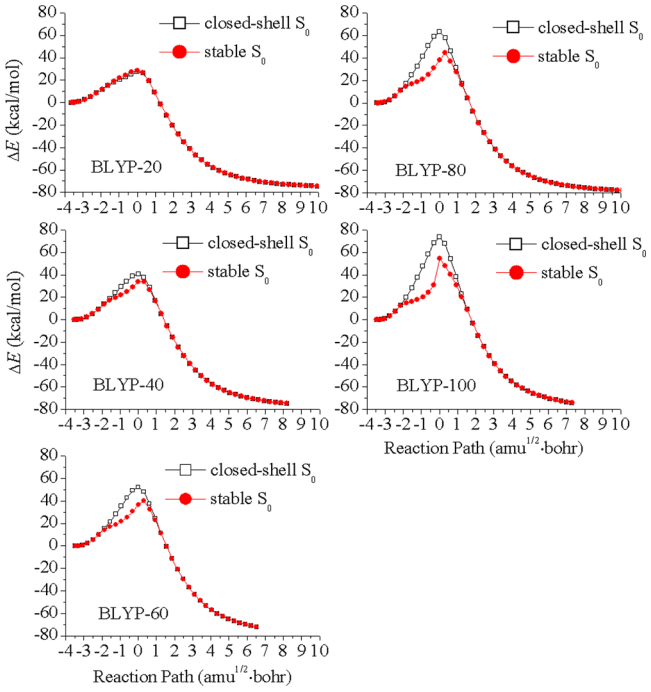

Figure 2. The comparison of the PECs of the closed-shell S_0 and the stable S_0 states. See Table 1 for the definition of the computaional methods.

solutions. The amount of HF exchange characterizing the 17 density functionals employed in ref 5 is listed in Table S1. The five best functionals, MPWB1K, MPW1K, MPW1B95, PBE1PBE, and PBE1KCIS, as stated in ref 5 are either H-GGA or HM-GGA ones which have at least 22% HF exchange. The restricted Kohn−Sham determinant for the last three are almost stable, whereas the first two are obviously unstable, as clearly shown in Figure S1. In particular, the MPWB1K functional, featuring 44% HF exchange, gives unstable restricted solutions. Because this functional was employed to calculate the PECs of ground and excited states in ref 5, the reliability of the PECs of ground and excited states using this functional can be doubted. We have calculated the PECs of the T_0 state using stable Kohn−Sham wave functions along the closed-shell S_0 IRCs by the five functionals of ref 5 with the aug-cc-pVDZ basis set. As shown in Figure S1, there are no crossings of the stable S_0 and T_0 PECs. However, da Silva and da Silva observed double crossings at the computational level of MPWB1K/aug-cc-pVDZ//MPWKCIS/cc-pVDZ. We calculated the stable T_0 PEC at the same level, which indeed double-crosses with the PEC of the closed-shell S_0 state but not the stable S_0 PEC, as clearly show in Figure S2. The double crossings, we suggest, are artificially formed by using the different computational level of optimization and single-point energy and unstable wave function.

We have also calculated the stable T_0 PECs along the closed-shell S_0 IRCs using the BLYP-X functionals in Table 1. The energy profiles of the stable T_0 and closed-shell S_0 states, and the ones of the stable T_0 and stable S_0 states, are summarized in Figures 3 and S4, respectively. As shown in Figure 3, the T_0 PEC does not cross the S_0 PEC in the B3LYP calculation. The smallest energy gap between these states is about 6 kcal/mol. Remember that the B3LYP functional gives an almost stable S_0 description for this reaction (see Figure 2). However, with an increasing amount of HF exchange, the restricted Kohn−Sham wave function tends to be more unstable, and the PECs of the closed-shell S_0 and stable T_0 states exhibit a double cross. Actually, the emergence of the double S_0−T_0 crossings is the consequence of using the unstable closed-shell wave function. Most probably, this is also one of the reasons for the double crossings observed in ref 5. The more important origin of the double S_0−T_0 crossings in ref 5 comes from the different computational level of optimization and single-point energy. In passing, we suggest that the S_1 and T_1 PECs calculated by time-dependent (TD) DFT methods based on the unstable reference state in ref 5 cannot be trusted. We note that when the PEC of the T_0 state is calculated on the basis of the stable S_0 IRC, the situation is different. As described in Figure S4, the

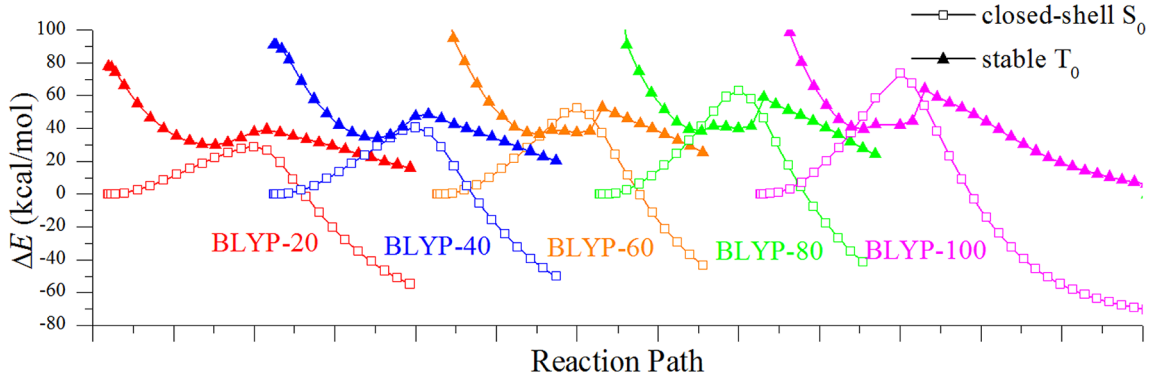

Figure 3. The energy profiles of the closed-shell S_0 and stable T_0 states calculated using the DFT methods with a different percentage of HF exchange (see Figure S3 with specific reaction path).

dx.doi.org/10.1021/ct3006562 | J. Chem. Theory Comput. 2012, 8, 4359−4363

PECs of the stable S_0 and the T_0 states get closer along with the increasing amount of HF exchange, and they are sometimes degenerate in some areas. However, no S_0−T_0 double crossings appear.

Then, unrestricted open-shell calculations using the DFT functional listed in Table 1 were employed to reinvestigate the decomposition of 1,2-dioxetanone. As a matter of fact, all of these calculations predict a stepwise biradical mechanism, characterized by two TSs and one intermediate (Int) between the two TSs, as shown in Figure 4. The expectation value over

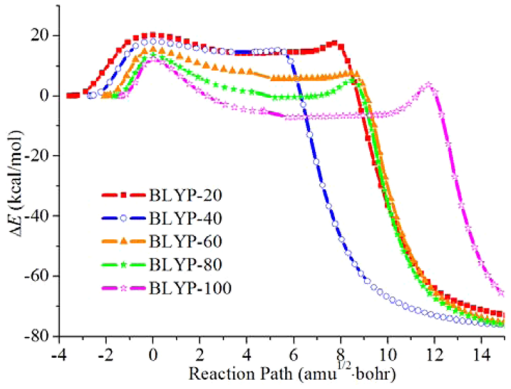

Figure 4. The energy profiles of the S_0 state calculated by the open-shell DFT methods with different amounts of HF exchange.

the total spin operator of those points between the two TSs is around 1 ($\langle S^2 \rangle \approx 1$), which indicates the existence of a biradical. This is in qualitative agreement with the mechanism proposed by multiconfigurational calculations in ref 3. For each calculation, the activation barrier of the second TS (TS2) is always lower than the first one (TS1), as shown in Figure 4. Hence, the TS1 barrier determines the reaction rate. The ΔG values of TS1 are summarized in Table 1. In contrast with the concerted mechanism, the reaction barrier decreases with the increasing amount of HF exchange (see Table 1 and Figure 4) and is comprised between 17.5 and 10.1 kcal/mol. As shown in Figure S5, all the unrestricted open-shell S_0 Kohn−Sham wave functions are virtually stable during the whole reaction no matter how high the percentage of HF exchange included in the exchange functional. The T_0 PECs based on the open-shell S_0 IRC paths are also calculated and presented in Figures 5 and S5 together with the S_0 PECs. As shown in Figure 5, the T_0 state is nearly degenerate with the stable S_0 state in the biradical region (their energy gap is actually no more than 1 kcal/mol). This result qualitatively agrees with the result of multiconfigurational calculation in ref 3. The "remains" of a continuous seam of intersection between S_0 and T_1 in ref 5 is mainly due to a situation where the S_0 potential energy surface is computed with a different method and therefore changes shape.

The experimental activation barriers of the decomposition of 1,2-dioxetane derivatives is known to be roughly in the range of 16−24 kcal/mol.[4] As Table 1 shows, the barriers calculated using open-shell and closed-shell B3LYP methods look reasonable and are consistent with the results obtained with direct optimization of the reduced two-particle matrixes reported in ref 2. However, the other closed-shell calculations performed with functionals including larger amounts of HF exchange show much larger barriers, because the associated Kohn−Sham wave functions are not stable. Moreover, because the activation barriers calculated by the open-shell method are always lower than the corresponding one calculated by the closed-shell method, the stepwise biradical decomposition is more favorable.

As a final note, we also compared the S_0 and T_0 PECs in the gas phase and solvents for both concerted and stepwise biradical mechanisms at the computational level of B3LYP/aug-cc-pVDZ//B3LYP/aug-cc-pVDZ. As described in Figure S6, the solvent effect hardly affects the PECs, so the solvent effect does not change our above conclusion qualitatively.

CONCLUSION

The proposed concerted and stepwise biradical decomposition mechanisms of 1,2-dioxetanone have been reinvestigated using DFT methods including different HF exchange functionals. The calculated results indicate that the closed-shell S_0 calculations with a large amount of HF exchange are unreliable due to the instability of the Kohn−Sham wave function. As a result, the appearance of the double crossings between the S_0 and T_0 PECs is a computational artifact. The open-shell DFT calculations predict a stepwise biradical mechanism, whose characteristics are qualitatively consistent with the conclusion drawn by the previously reported state-of-the-art ab initio calculations.

ASSOCIATED CONTENT

Supporting Information

HF percentage of different functionals employed in ref 5; comparison of the PECs of the closed-/open-shell S_0, stable S_0, and T_0 states; comparison of the S_0 and T_0 PECs in the gas phase and solvents; Cartesian coordinates of all stable

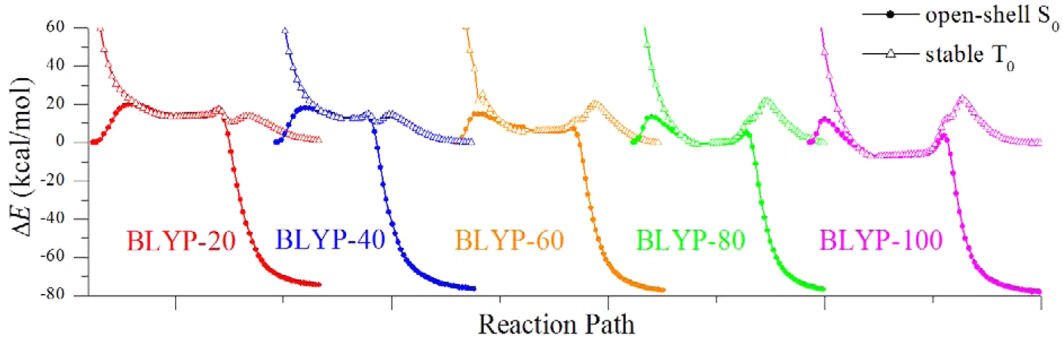

Figure 5. The energy profiles of the stable S_0 and stable T_0 states calculated by the DFT methods with different percentages of HF exchange (see Figure S4 with specific reaction path).

dx.doi.org/10.1021/ct3006562 | J. Chem. Theory Comput. 2012, 8, 4359−4363

structures. This material is available free of charge via the Internet at http://pubs.acs.org.

AUTHOR INFORMATION

Corresponding Author

*E-mail: yajun.liu@bnu.edu.cn (Y.-J.L).

Notes

The authors declare no competing financial interest.

ACKNOWLEDGMENTS

This work was supported by grants from the National Natural Science Foundation of China (Grant Nos. 21073017 and 21273021) and the Major State Basic Research Development Programs (Grant No. 2011CB808500). R.L. thanks the Swedish Research Council (VR) for financial support. D.R.-S. thanks the European Research Council under the European Community's Seventh Framework Programme (FP7/2007-2013)/ERC grant agreement no. 255363.

REFERENCES

(1) Koo, J.-Y.; Schuster, G. B. *J. Am. Chem. Soc.* **1977**, *99*, 6107−6109.
(2) (a) Greenman, L.; Mazziotti, D. A. *J. Chem. Phys.* **2010**, *133*, 164110. (b) Greenman, L.; Mazziotti, D. A. *J. Chem. Phys.* **2011**, *134*, 174110−174118.
(3) Liu, F.; Liu, Y.-J.; Vico, L. D.; Lindh, R. *J. Am. Chem. Soc.* **2009**, *131*, 6181−6188.
(4) Yue, L.; Liu, Y.-J.; Fang, W.-H. *J. Am. Chem. Soc.* **2012**, *134*, 11632−11639.
(5) da Silva, L. P.; da Silva, J. C. G. E. *J. Comput. Chem.* **2012**, *33*, 2118−2123.
(6) Roca-Sanjuán, D.; Lundberg, M.; Mazziotti, D. A.; Lindh, R. *J. Comput. Chem.* **2012**, *33*, 2124−2126.
(7) da Silva, L. P.; da Silva, J. C. G. E. *J. Comput. Chem.* **2012**, *33*, 2127−2130.
(8) Becke, A. D. *Chem. Phys.* **1993**, *98*, 5648−5652.
(9) (a) Vosko, S. H.; Wilk, L.; Nusair, M. *Can. J. Phys.* **1980**, *58*, 1200−1211. (b) Lee, C.; Yang, W.; Parr, R. G. *Phys. Rev. B: Condens. Matter* **1988**, *37*, 785−789. (c) Stephens, P. J.; Devlin, F. J.; Chabalowski, C. F.; Frisch, M. J. *J. Phys. Chem.* **1994**, *98*, 11623−11627.
(10) (a) Seeger, R.; Pople, J. A. *J. Chem. Phys.* **1977**, *66*, 3045−3050. (b) Bauernschmitt, R.; Ahlrichs, R. *J. Chem. Phys.* **1996**, *104*, 9047−9052.
(11) (a) Barone, V.; Cossi, M. *J. Phys. Chem. A* **1998**, *102*, 1995−2001. (b) Cossi, M.; Rega, N.; Scalmani, G.; Barone, V. *J. Chem. Phys.* **2001**, *114*, 5691.
(12) Cossi, M.; Rega, N.; Scalmani, G.; Barone, V. *J. Comput. Chem.* **2003**, *24*, 669−681.
(13) (a) Dunning, T. H. *J. Chem. Phys.* **1989**, *90*, 1007−1023. (b) Kendall, R. A.; Dunning, T. H.; Harrison, R. J. *J. Chem. Phys.* **1992**, *96*, 6796−6806. (c) Woon, D. E.; Dunning, T. H. *J. Chem. Phys.* **1993**, *98*, 1358−1371.
(14) Frisch, M. J.; Trucks, G. W.; Schlegel, H. B.; Scuseria, G. E.; Robb, M. A.; Cheeseman, J. R.; Scalmani, G.; Barone, V.; Mennucci, B.; Petersson, G. A.; Nakatsuji, H.; Caricato, M.; Li, X.; Hratchian, H. P.; Izmaylov, A. F.; Bloino, J.; Zheng, G.; Sonnenberg, J. L.; Hada, M.; Ehara, M. T., K.; Fukuda, R.; Hasegawa, J.; Ishida, M.; Nakajima, T.; Honda, Y.; Kitao, O.; Nakai, H.; Vreven, T.; Montgomery, J. A., Jr.; Peralta, J. E.; Ogliaro, F.; Bearpark, M.; Heyd, J. J.; Brothers, E.; Kudin, K. N.; Staroverov, V. N.; Kobayashi, R.; Normand, J.; Raghavachari, K.; Rendell, A.; Burant, J. C.; Iyengar, S. S.; Tomasi, J.; Cossi, M.; Rega, N.; Millam, N. J.; Klene, M.; Knox, J. E.; Cross, J. B.; Bakken, V.; Adamo, C.; Jaramillo, J.; Gomperts, R.; Stratmann, R. E.; Yazyev, O.; Austin, A. J.; Cammi, R.; Pomelli, C.; Ochterski, J. W.; Martin, R. L.; Morokuma, K.; Zakrzewski, V. G.; Voth, G. A.; Salvador, P.; Dannenberg, J. J.; Dapprich, S.; Daniels, A. D.; Farkas, Ö.; Foresman, J. B.; Ortiz, J. V.; Cioslowski, J.; Fox, D. J. *Gaussian 09*, revision A.02; Gaussian, Inc.: Wallingford, CT, 2009.